ACS Infectious Diseases

pubs.acs.org/journal/aidcbc

Article

Comparative Kinetic Analysis of OXA-438 with Related OXA-48-Type Carbapenem-Hydrolyzing Class D β-Lactamases

Denise De Belder, Barbara Ghiglione, Fernando Pasteran, Juan Manuel de Mendieta, Alejandra Corso, Lucrecia Curto, Adriana Di Bella, Gabriel Gutkind, Sonia A. Gomez, and Pablo Power*

Cite This: https://dx.doi.org/10.1021/acsinfecdis.0c00537

Read Online

ACCESS | Metrics & More | Article Recommendations | Supporting Information

ABSTRACT: Novel variants of OXA-48-type enzymes with the ability to hydrolyze oxyimino-cephalosporins and carbapenems are increasingly reported. Since its first report in 2011, OXA-163 is now extensively spread throughout Argentina, and several variants like OXA-247 have emerged. Here, we characterized a new $bla_{OXA-48-like}$ variant, OXA-438, and we performed a comparative kinetic analysis with the local variants OXA-247 and OXA-163 and the internationally disseminated OXA-48. $bla_{OXA-163}$, $bla_{OXA-247}$, and $bla_{OXA-438}$ were located in a 70 kb $IncN_2$ conjugative plasmid. OXA-438 presented mutations in the vicinity of conserved KTG (214−216), with a 2-aa deletion (R220-I221) and a D224E shift (as in OXA-163) compared to OXA-48. Despite Kpn163 (OXA-163), Kpn247 (OXA-247) and Eco438 (OXA-438) were resistant to meropenem and ertapenem, and the transconjugants (TC) remained susceptible (however, the carbapenems minimum inhibitory concentrations were ≥3 times 2-fold dilutions higher than the acceptor strain). TC163 and Eco48 were resistant to oxyimino-cephalosporins, unlike TC247 and TC438. k_{cat}/K_m values for cefotaxime in OXA-163 were slightly higher than the rest of the variants that were accompanied by a lower K_m for carbapenems. For OXA-163, OXA-247, and OXA-438, the addition of $NaHCO_3$ improved k_{cat} values for both cefotaxime and ceftazidime; carbapenems k_{cat}/K_m values were higher than for oxyimino-cephalosporins. Mutations occurring near the conserved KTG in OXA-247 and OXA-438 are probably responsible for the improved carbapenems hydrolysis and decreased inactivation of oxyimino-cephalosporins compared to OXA-163. Dichroism results suggest that deletions at the $\beta5-\beta6$ loop seem to impact the structural stability of OXA-48 variants. Finally, additional mechanisms are probably involved in the resistance pattern observed in the clinical isolates.

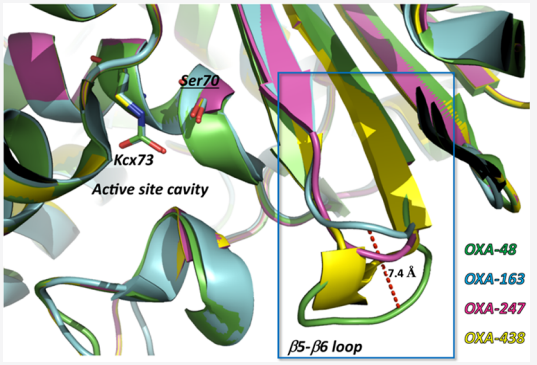

KEYWORDS: *carbapenemases, $\beta5-\beta6$ loop, sodium bicarbonate, oxyimino-cephalosporins, OXA-163*

Downloaded via Pablo Power on October 2, 2020 at 18:24:35 (UTC).
See https://pubs.acs.org/sharingguidelines for options on how to legitimately share published articles.

Class D or OXA-type enzymes are represented by more than 800 diverse enzymes according to the National Center for Biotechnology Information (NCBI) database (https://www.ncbi.nlm.nih.gov/pathogens/beta-lactamase-data-resources/) or the β-Lactamase Database (BLDB; http://bldb.eu/BLDB.php?prot=D),[1] respectively. This heterogeneous group comprises chromosome- and plasmid-encoded enzymes, with some members possessing <20% sequence identity.[2−4] Carbapenem-hydrolyzing class D β-lactamases (CHDL) belong to a subgroup that is widespread and are among the main causes of carbapenem resistance within *A. baumannii* and *Enterobacterales*.[5]

OXA-48 was the first described enzyme from this subgroup and possesses a high catalytic efficiency for imipenem as compared to other close relatives, but low activity for oxyimino-cephalosporins with undetectable activity for ceftazidime.[4] Since the first description of OXA-48, an increasing number of allelic variants have been described.[6−8] These OXA-48-like enzymes differ from OXA-48 by a few amino-acid substitutions and deletions.[9] Among them, OXA-163 has been only detected in *Enterobacterales* from Argentina and Egypt.[5] As this variant has reduced ability to hydrolyze carbapenems but regains activity toward ceftazidime compared to OXA-48,[4,10] its inclusion as a CHDL can be argued. This behavior has been attributed to a single Ser220Asp substitution and a four amino-acid deletion (222-ArgIleGluPro-225) compared to OXA-48 (according to DBL numbering).[11,12] The Ser220Asp substitution is located at the C-terminal segment of the $\beta5$ strand, and the four amino-acid deletion is in the loop region between the $\beta5$ and $\beta6$ strands.[4] The $\beta5$ strand forms one side of the active-site cavity and contains the conserved motif K(S/T)G (residues 216−218) typical for class D β-lactamases (DBLs), and the loop between $\beta5-\beta6$ strands has been suggested to be important for the ability

Received: July 28, 2020
Published: September 24, 2020

© XXXX American Chemical Society

Table 1. Minimum Inhibitory Concentrations (μg/mL) of Clinical Strains and *E. coli* Transconjugants Producing OXA-48 Variants

	clinical isolates			transconjugants			acceptor
antibiotics	*E. coli* ECO438	*K. pneumonia* KPN163	*K. pneumonia* KPN247	*E. coli* TC438	*E. coli* TC163	*E. coli* TC247	*E. coli* J53
ampicillin	1024	>1024	>1024	1024	1024	>1024	≤4
cephalothin	256	>1024	256	64	256	32	16
cefotaxime	0.5	128	1	0.5	16	0.125	0.03
ceftazidime	2	256	32	2	64	4	0.125
imipenem	8	1	8	0.5	0.125	0.5	0.125
meropenem	2	8	8	0.125	0.06	0.125	0.03
ertapenem	16	>32	>32	0.06	1	0.03	0.004

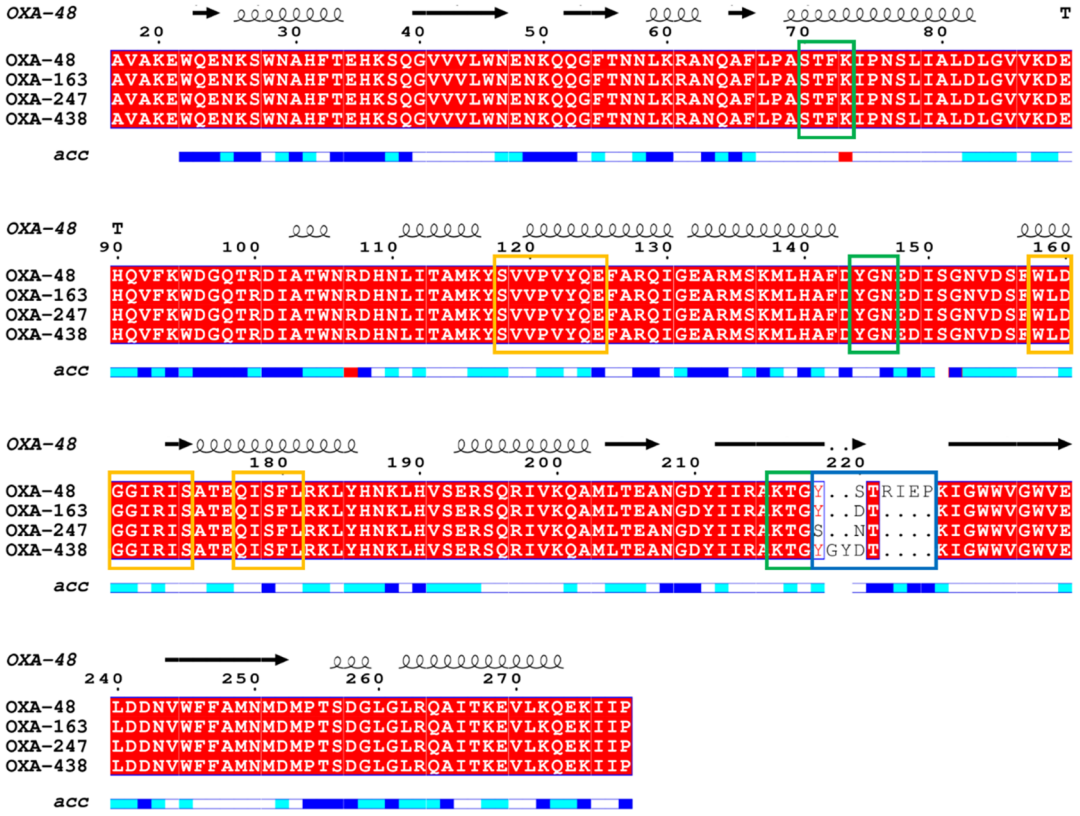

Figure 1. Sequence analysis of OXA-48 variants. Multialignment of amino acid sequences of novel OXA-438 and OXA-247 and other OXA-48 variants, using the standard numbering scheme for OXA-48. The location of α-helices and β-sheets is indicated in the upper side (taken from PDB 3HBR) and relative solvent accessibility in the bottom (blue, highly accessible; cyan, poorly accessible; white, hidden or nonaccessible). Amino acid motifs that are well conserved among class D β-lactamases are indicated by green (active site conserved motifs) and orange (other conserved motifs) boxes. The $\beta5-\beta6$ region containing the mutations in OXA-48 variants is indicated by a blue box. The figure was prepared using Espript (http://espript.ibcp.fr/ESPript/ESPript/).

of an OXA-variant to hydrolyze carbapenems; therefore, the deletion by itself may impact carbapenem hydrolysis.[10,13]

Recently, novel variants of the OXA-48-like enzymes ($bla_{OXA-247}$ and $bla_{OXA-438}$) with the ability to hydrolyze oxyimino-cephalosporins and carbapenems emerged in Argentina.[14] The $bla_{OXA-438}$ variant was detected to form an *E. coli* isolated from the urine of a pediatric patient suffering from B-cell acute lymphoblastic leukemia, which was phenotypically resistant to carbapenems and susceptible to oxyimino-cephalosporins. The aim of this work was to characterize this new variant and to comparatively evaluate the hydrolytic behavior of OXA-247 and OXA-438.

RESULTS AND DISCUSSION

Epidemiological Data and β-Lactamase PCR Results. *Escherichia coli* M17224 (ECO438) was isolated in 2014 from the urine of a pediatric patient suffering from B-cell acute lymphoblastic leukemia, with a history of multiple hospitalizations and antimicrobial treatments due to recurrent *E. coli* infections. ECO438 was phenotypically resistant to carbapenems, but all the biochemical and colorimetric hydrolytic tests done to confirm carbapenemase activity gave negative results as well as the ESBL screening, despite an immunochromatographic test giving a positive signal for OXA-163.[15]

Polymerase chain reactions (PCRs) were negative for bla_{KPC}, bla_{AmpC}, and bla_{OXA-1} but positive for $bla_{OXA-48-like}$. The new allele was assigned as $bla_{OXA-438}$ by NCBI (https://www.ncbi.nlm.nih.gov/pathogens/submit-beta-lactamase/). The epidemiological

https://dx.doi.org/10.1021/acsinfecdis.0c00537
ACS Infect. Dis. XXXX, XXX, XXX−XXX

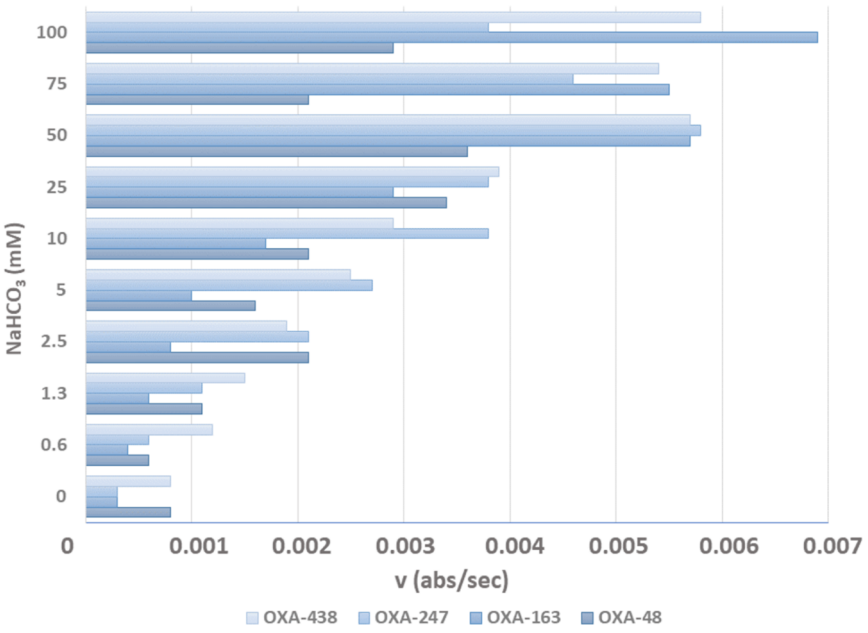

Figure 2. Effect of sodium bicarbonate on the OXA activity. The initial rates of hydrolysis of nitrocefin were determined under different concentrations of sodium bicarbonate.

and phenotypic data of *Klebsiella pneumoniae* M11969 (KPN163) and *K. pneumoniae* M13056 (KPN247) were described in a previous work.[14]

Susceptibility Profiles. Minimum inhibitory concentration (MIC) results revealed that the isolate ECO438 harboring the new variant OXA-438 was resistant to penicillins and susceptible to oxyimino-cephalosporins and showed low-level resistance to carbapenems (Table 1). In contrast, the other local variants, KPN163 (OXA-163) and KPN247 (OXA-247), were resistant to oxyimino-cephalosporins (KPN247 reduced susceptibility to cefotaxime) and exhibited higher MIC values to ertapenem (Table 1).

Plasmid Characterization and Genetic Environment. The $bla_{OXA-438}$ gene was successfully transferred by biparental conjugation, demonstrating the mobilization capacity of the $bla_{OXA-438}$-harboring plasmid, like the previously characterized $bla_{OXA-163}$ and $bla_{OXA-247}$ genes.[14]

Susceptibility results of ECO438 transconjugant (TC438) were compared with those of the acceptor strain *E. coli* J53. TC438 was resistant to penicillins and susceptible to oxyimino-cephalosporins but was ≥3 times 2-fold dilutions higher compared with the acceptor strain *E. coli* J53. Carbapenem MICs of TC438 were interpreted as susceptible; however, ertapenem was ≥3 times 2-fold dilutions higher compared with the acceptor strain *E. coli* J53. Overall, the phenotypic characteristics of TC438 suggest the occurrence of transference of the $bla_{OXA-438}$ plasmid. Susceptibility results of TC163 and TC247 suggested the transference of bla_{OXA}[14] (Table 1). Briefly, TC163 and TC247 showed resistance to penicillins, variable MICs to oxyimino-cephalosporins, and susceptibility to carbapenems, but ertapenem showed ≥3 times 2-fold dilutions compared with the acceptor strain *E. coli* J53.

S1 nuclease showed that ECO438 harbored at least 5 plasmids, and three of them were transferred to TC438 (Figure S1). PCR of TC438 confirmed the presence of $bla_{OXA-438}$ only. OXA-163 and OXA-247 harbored a ca. 70 kb plasmid, as previously reported.[14] KPN163, KPN247, ECO438, and corresponding TCs shared a ca. 70 kb plasmid (Figure S1). Additionally, the clinical isolates KPN163, KPN247, and ECO438 as well as the transconjugants were confirmed to carry an $IncN_2$ plasmid.

An analysis of the $bla_{OXA-438}$ genetic environment revealed that this gene was inserted into a structure identical to that found in $bla_{OXA-163}$ and $bla_{OXA-247}$.[10,14] Briefly, $bla_{OXA-438}$ was bracketed upstream by the insertion sequence IS*4321* and downstream by a truncated IS*4*-like element (Figure S2). Altogether, these results suggest that these enzymes might be carried on highly similar plasmids.

OXA-48 Variants Harbor Amino Acid Modifications at the KTG-Associated Loop. The new variants OXA-247 and OXA-438 were derived from OXA-48 by mutations occurring in the vicinity of the conserved motif KTG, specifically in the region spanning the $\beta5-\beta6$ loop, as observed in Figure 1 and previously reported.[10,13] Also, the alignment shows that the organization of the active site of OXA-438 seems to be conserved compared to other OXA-48-derived enzymes, including the conserved motifs SerThrPheLys (70−73), TyrGlyAsn (144−146), and LysThrGly (216−218). OXA-163 differs from OXA-48 by the presence of a single amino acid modification Ser220Asp and the deletion of Arg222−Ile223−Glu224−Pro225.[10] OXA-247 contains the same 4-residue deletion as OXA-163 and two substitutions Tyr219Ser and Ser220Asn compared to OXA-48.[14] Finally, OXA-438 exhibited these same modifications and the insertion of two residues between Tyr219−Asp220, according to the alignment. These mutations are likely to result in modifications in the folding of the $\beta5-\beta6$ loop, leading to a local impact on the enzyme structure. Crystal structures will allow us to better evaluate which is the actual role of $\beta5-\beta6$ mutations and the tridimensional arrangement of the residues involved.

Effect of Sodium Bicarbonate on the β-Lactamase Activity. Upon the first report of the presence of an *N*-carboxylated lysine residue in OXA-10,[16] Golemi et al. demonstrated that this residue has a critical role in the reaction mechanism of OXA-10, participating in a base in the active site of the enzyme.[17] In this paper, the presence of sodium

https://dx.doi.org/10.1021/acsinfecdis.0c00537
ACS Infect. Dis. XXXX, XXX, XXX−XXX

Table 2. Steady-State Kinetic Parameters of OXA-48 Variants in the Presence of 50 mM Sodium Bicarbonate[a]

enzyme	parameter	nitrocefin	cefotaxime	ceftazidime	imipenem	meropenem	ertapenem
OXA-48	K_m (μM)	60 ± 3	174 ± 14	9900 ± 740	2.3 ± 0.07	0.06 ± 0.002	0.2 ± 0.003
	k_{cat} (s^{-1})	430 ± 8	<0.001	NH	5 ± 0.3	0.12 ± 0.001	0.03 ± 0.002
	k_{cat}/K_m (μM^{-1} s^{-1})	7.2 ± 0.5	$<6 \times 10^{-6}$	ND	2.0 ± 0.2	1.9 ± 0.1	0.2 ± 0.03
OXA-163	K_m (μM)	35 ± 3	19 ± 1	9200 ± 276	0.03 ± 0.001	0.06 ± 0.002	0.06 ± 0.004
	k_{cat} (s^{-1})	243 ± 8	0.004	NH	0.06 ± 0.003	0.06 ± 0.003	0.01 ± 0.001
	k_{cat}/K_m (μM^{-1} s^{-1})	6.9 ± 0.8	2×10^{-4}	ND	1.9 ± 0.1	1.0 ± 0.1	0.2 ± 0.03
OXA-247	K_m (μM)	50 ± 6	395 ± 35	>10000	3.4 ± 0.1	0.6 ± 0.02	1.4 ± 0.03
	k_{cat} (s^{-1})	274 ± 12	<0.001	NH	0.8 ± 0.04	0.18 ± 0.01	0.08 ± 0.004
	k_{cat}/K_m (μM^{-1} s^{-1})	5.5 ± 0.8	$<3 \times 10^{-6}$	ND	0.2 ± 0.02	0.3 ± 0.04	0.1 ± 0.02
OXA-438	K_m (μM)	40 ± 3	68 ± 2	>10000	1.9 ± 0.05	0.07 ± 0.001	0.16 ± 0.007
	k_{cat} (s^{-1})	332 ± 9	<0.001	NH	8 ± 0.5	0.06 ± 0.003	0.03 ± 0.002
	k_{cat}/K_m (μM^{-1} s^{-1})	8.3 ± 0.8	2×10^{-5}	ND	4.4 ± 0.5	0.9 ± 0.09	0.2 ± 0.03

[a]ND, not determined; NH, no hydrolysis was observed under the used experimental conditions.

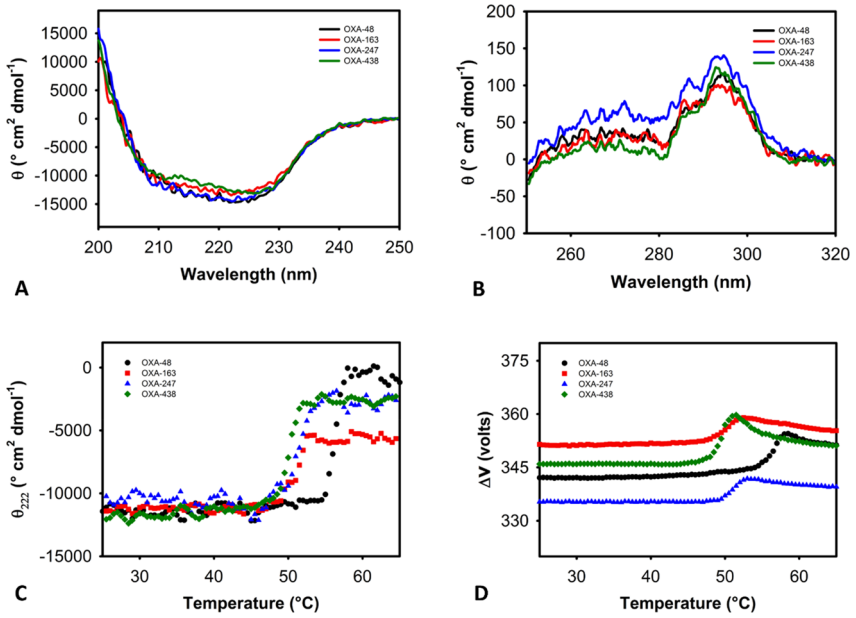

Figure 3. UV-circular dichroism (CD) and thermal denaturation spectra. Top: (A) far UV CD and (B) near UV CD spectra for OXA-48 variants. Bottom: (C) thermally induced unfolding transitions were monitored by the evolution of the molar ellipticity at 222 nm and (D) values of the dynode voltage at each condition.

bicarbonate in the reaction mix was utilized to provide the necessary amount of CO_2 to yield *N*-carboxylation of Lys73. To evaluate the effect of sodium bicarbonate on the activity of OXA-48 variants, we determined the hydrolysis rate of nitrocefin in the presence of increasing concentrations of the salt. The general behavior of all four variants of OXA-48 reflects that, upon increasing concentrations of CO_2, the enzyme shows a stronger hydrolysis rate over nitrocefin (Figure 2). Overall, the maximum activity was achieved with 50 mM sodium bicarbonate, which is probably a saturating concentration; higher concentrations up to 100 mM $NaHCO_3$ were generally detrimental in the hydrolysis rate, except for OXA-163, which showed a 1.2-fold increase in the activity. Consequently, in this study, we performed kinetic reactions using 50 mM $NaHCO_3$ in the reaction buffer, which is coincidental with that used in previous studies.[2,17]

Only OXA-48 and OXA-438 showed activity in absence of sodium bicarbonate, with the hydrolysis rate 4.5- and 7-fold lower than the activity obtained with 50 mM $NaHCO_3$, respectively. Interestingly, OXA-163 was less active than the other variants in the 0.625−25 mM $NaHCO_3$ range, which suggests that the activity in this variant could be more sensitive to minor changes in CO_2 concentrations within the active site, and it is evident that, from 50 mM bicarbonate, the activity resumes as in the rest of the OXA variants.

Comparative Kinetic Behavior of OXA-438 with OXA-48-Type Enzymes and Redefinition of the Carbapenemase Activity. Steady-state kinetic parameters were determined in the presence of 50 mM sodium bicarbonate (Table 2).

The kinetic behavior of all four OXA β-lactamases was similar for nitrocefin, showing both high turnover (k_{cat}) and catalytic efficiency (k_{cat}/K_m) values. The four OXA variants showed different behaviors toward the oxyimino-cephalosporins cefotaxime and ceftazidime. For cefotaxime, K_m values showed that OXA-163 can have the highest affinity for Michaelis complex formation, compared to the high K_m values in OXA-247 and OXA-48. However, compared to OXA-48, OXA-163 showed a slight improvement in the ability to hydrolyze cefotaxime, albeit both the k_{cat} and k_{cat}/K_m values are almost insignificant to be considered as biologically relevant; the impossibility to accurately determine the k_{cat} and k_{cat}/K_m values for the other variants (k_{cat} values were assessed as <0.001 s^{-1}) relies on the fact that the high molar extinction coefficient for cefotaxime

https://dx.doi.org/10.1021/acsinfecdis.0c00537
ACS Infect. Dis. XXXX, XXX, XXX−XXX

(above 25000 M^{-1} cm^{-1} at 260 nm) yields absorbance values that are beyond the detection capacity of the spectrophotometer when V_{max} values were assayed. On the other hand, the K_m values obtained for ceftazidime in all four variants (close to 10 mM) are negligible in terms of biological significance, for which this antibiotic is not a substrate for OXA-48-related β-lactamases; this is supported by a nondetectable hydrolytic activity against ceftazidime upon direct incubation of the enzymes with the drug.

The K_m values obtained for the tested carbapenems (imipenem, meropenem, and ertapenem) were very low for all OXA enzymes (Table 2), which can be associated with a very high affinity. Both OXA-438 and OXA-48 showed the highest turnover (k_{cat}) for imipenem compared with the other enzymes. The catalytic efficiency values (k_{cat}/K_m) for imipenem were highest for OXA-438, followed by OXA-48 and OXA-163. Instead, for Meropenem, OXA-48 showed the highest k_{cat}/K_m values. Ertapenem was the most stable carbapenem against hydrolysis in all OXA-variants tested ($k_{cat}/K_m < 1$ M^{-1} s^{-1}). Finally, OXA-247 had the weakest carbapenemase hydrolytic activity ($k_{cat}/K_m < 1$ M^{-1} s^{-1}). In summary, OXA-438 and OXA-48 demonstrated the strongest imipenem- and Meropenem-hydrolyzing activity.

Deletions at the β5−β6 Loop Seem to Impact the Structural Stability of OXA-48 Variants. A biophysical characterization was carried out to evaluate the impact on amino acid substitutions, insertions, and deletions in each OXA variant. Even though slight differences were observed, far UV circular dichroism (CD) spectra (Figure 3 A and B) indicated preserved secondary structure content for all OXA variants (panel A). Accordingly, near UV-CD showed some modifications in the tertiary structure of the variants (panel B). The observed differences in the content of the tertiary structure could be attributed at least in part to the deletions in OXA-163, OXA-247, and OXA-438 compared to OXA-48; however, OXA-247 seems to be the variant with a different behavior that could be explained by the spatial rearrangements of the polypeptide chain due to modifications in the amino acid sequence.

To understand if the observed changes lead to alterations in the global stability, the thermal denaturation profile was obtained (Figure 3 C and D). For each protein, the evolution of the elipticity at 222 nm (minima observed in the spectra shown in Figure 3C) was measured as a function of temperature while the evolution of the dynode voltage was recorded simultaneously (Figure 3D). An increase in the latter value reveals the appearance of protein aggregates, therefore indicating that thermal-induced aggregation occurred concomitantly with the loss of the secondary structure.[18] In such cases, the temperature at the onset of aggregation (T_o) was obtained as an assessment of protein stability.[19] The observed T_o values were 54 °C (OXA-48), 49 °C (OXA-163), 48 °C (OXA-247), and 47 °C (OXA-438). Interestingly, OXA-48 proved to have the highest stability, with its T_o up to 7 °C higher than the other enzymes. Whether these results are correlated with the activities observed in the absence of sodium bicarbonate remains to be determined with further studies.

CONCLUSIONS

In this study we characterized a carbapenem resistant clinical isolate *Escherichia coli* M17224 (ECO438) obtained from a pediatric patient suffering from leukemia. ECO438 was negative for all the prevalent carbapenemases but harbored a novel variant of $bla_{OXA\text{-}48\text{-}like}$ located in a ca. 70 kb IncN2 plasmid. Moreover, in this work we performed biochemical and molecular studies to understand the role of mutations occurring at the β5−β6 loop in OXA-247 and OXA-438 on the hydrolytic behavior of OXA β-lactamases. We propose that alterations in the architecture and folding of this loop, which is close to the conserved KTG motif, modify the hydrolytic behavior on OXA-48-type β-lactamases and have a strong impact on the overall structural stability. Further experimental structural studies are being conducted to better determine this hypothesis.

Judging by the susceptibility behavior of OXA-producing strains and the observed hydrolytic activity of the enzymes, additional mechanisms such as reduced permeability through specific porins and/or active efflux may be involved in the overall resistance pattern. This is evidenced, for example, with imipenem, for which there is a 10-fold reduction in the catalytic efficiency albeit a reduced susceptibility in the producing strains is achieved. Therefore, the influence of these additional mechanisms cannot be ruled out and deserves further analysis.

The analysis of the available kinetic data in the literature for several OXA β-lactamases raises the fact that kinetic experiments have often been performed without supplementing the reaction mixture with a CO_2 source (i.e., sodium bicarbonate), which is needed for lysine *N*-carboxylation. In these conditions (absence of bicarbonate), partial *N*-carboxylation of the active-site lysine during *in vitro* experiments is usually achieved, leading to nonconsistent kinetic parameters (and therefore questionable results) due to the presence of inactive enzymes in the mixture; this was already suggested by Antunes et al.,[2] where several studies are suggested for reference. We also demonstrated that the activity of the OXA enzymes (or at least those studied in this work) is strongly dependent on the bicarbonate concentration, suggesting that a 50 mM concentration can be used as standard amount during kinetic analysis. If we consider that the *in vivo* concentration of carbon dioxide was reported to be around 1.3 mM,[20] it is expected that the OXA β-lactamases will be fully carbamylated in bacteria, and the discrepancies that might be observed between the *in vitro* analysis and the *in vivo* behavior will be strongly dependent on the experimental conditions used, i.e., the presence or absence of a carbon dioxide source.

METHODS

Bacterial Strains. Clinical isolates suspicious of OXA-48-like production were referred to the National Reference Laboratory in Antimicrobial Resistance (NRLAR) for further characterization due to intermediate or resistance phenotypes to ertapenem, resistance to piperacillin/tazobactam (Clinical and Laboratory Standards Institute, CLSI 2018),[21] and susceptibility to imipenem and to third- and fourth-generation cephalosporins (http://antimicrobianos.com.ar/ATB/wp-content/uploads/2014/10/ALGORITMOS-MAX-Y-MINIMO.pdf).

The isolates used in this study were: *E. coli* M15260 (ECO48), an OXA-48-producing isolate kindly provided by Dr. Roberto Melano (Public Health Ontario, Canada); previously characterized *K. pneumoniae* M11969 (KPN163), an OXA-163 producer; *K. pneumoniae* M13056 (KPN247), an OXA-247 producer;[14] and *E. coli* M17224 (ECO438), the new variant OXA-438 producer. *E. coli* DH5α and *E. coli* TOP10 were used to clone $bla_{OXA\text{-}type}$ genes. Sodium azide resistant *E. coli* J53 was used as the recipient strain in conjugation assays; *E. coli* BL21(DE3) (Novagen, USA) was used to induce the expression of $bla_{OXA\text{-}48\text{-}like}$ genes.

Identification, Antimicrobial Susceptibility Assays, and PCR Detection of Relevant Genes. The isolates were

https://dx.doi.org/10.1021/acsinfecdis.0c00537
ACS Infect. Dis. XXXX, XXX, XXX−XXX

identified using matrix-assisted laser desorption ionization time-of-flight (MALDI-TOF) mass spectrometry (Bruker, Germany). Carbapenemase activity was screened with the Triton-Hodge,[22] Blue-Carba, and Carba-NP-Direct tests. Extended spectrum β-lactamases (ESBLs) screening was carried out using double disk synergy tests following CLSI recommendations.[21] The production of OXA-163-type enzymes was suspected using the immunochromatographic lateral flow assay and the OXA-163/48 Duo K-SeT test (Coris BioConcept).[15] Susceptibility testing was performed by broth microdilution (Microscan Walkaway, Beckman Coulter, Inc.) following CLSI guidelines and interpretation criteria (M100-S28, 2018)[21] to ampicillin, cefotaxime, cephalothin, ceftazidime, ceftazidime-avibactam, ertapenem, imipenem, and meropenem.

Biparental Conjugation and Plasmid Profile. Biparental conjugation was performed using a donor and recipient mix ratio of 1:3 and incubated overnight at 35 °C. Transconjugant cells were selected on LB agar plates containing ampicillin (50 μg/mL) plus sodium azide (200 μg/mL).[23] Plasmid content and their estimated sizes were determined by S1-nuclease digestion of genomic DNA followed by pulsed field gel electrophoresis (S1-PFGE).[24] Incompatibility groups were studied by PCR-based replicon typing (PBRT),[25,26] and specific PCR for $IncN_2$ (see Table S1).

***bla*$_{OXA48\text{-}like}$ Alleles and Genetic Environment.** *bla*$_{OXA\text{-}48\text{-}like}$ alleles were determined by PCR and Sanger sequencing with specific primers listed in Table S1. The genetic environment of *bla*$_{OXA\text{-}48\text{-}like}$ was studied by inverse PCR, as previously described.[10] Briefly, the total plasmid content was extracted from transconjugant cells with NucleoBond Xtra Midi (Macherey Nagel, Bethlehem, PA, USA) following the manufacturer's protocol. DNA restriction was done with *Hin*dIII and *Pst*I [New England Biolabs (NEB), Ipswich, MA, USA]. After restriction, the plasmid DNA was precipitated with LiCl and ligated with T4 DNA Ligase (NEB, Ipswich, MA, USA). pACyC and lambda phage DNA were used as controls. Ligated DNA was subjected to inverse PCR using outgoing primers detailed in Table S1. PCR products were run in a 1% agarose gel, and suspected bands were cut; the DNA was purified with a PCR cleanup gel extraction kit (Macherey Nagel, Bethlehem, PA, USA) and sequenced in an ABI 3500 genetic analyzer (Applied Biosystems, Foster City, CA, USA). The sequence analysis was performed using the BLAST program available at the National Center for Biotechnology Information Web site (http://www.ncbi.nim.nih.gov/). Multiple-sequence alignments were performed with Clustal Omega (http://www.ebi.ac.uk/Tools/msa/clustalo/) and BioEdit version 7.0.0. The insertion sequences were searched in the IS finder (https://www-is.biotoul.fr/blast.php.

Cloning and Expression of the *bla*$_{OXA\text{-}48\text{-}like}$ Genes. *bla*$_{OXA48\text{-}like}$ cloning was done using a CloneJet PCR cloning kit (Thermo Fisher Scientific). *bla*$_{OXA\text{-}48}$, *bla*$_{OXA\text{-}163}$, *bla*$_{OXA\text{-}247}$, and *bla*$_{OXA\text{-}438}$ were amplified by conventional PCR with primers that introduced restriction enzyme sites (*Nde*I and *Hin*dIII, see Table S1). Amplification fragments (ca. 780 bp) were cloned into pJET1.2/blunt vector (Thermo Scientific, Waltham, MA, USA) following the blunt-end cloning protocol and ligated with T4 DNA ligase. Prior to electroporation, DNA vectors were purified with an AccuPrep PCR Purification Kit (Bioneer, Oakland, CA). *Escherichia coli* DH5α cells were electroporated with the ligation product or control vectors in a Gene Pulser II electroporation system (BioRad, Hercules, CA, USA). Transformed cells were incubated for 1 h at 37 °C and plated onto 1.5% lysogeny broth (LB) agar with 50 μg/mL kanamycin and 1.6 ng/mL X-gal. The recombinant plasmids, pJET1.2/blunt-OXA (−48, −163, −247, and −438), were purified with an ADN Puriprep-P kit (Highway, Argentina). Plasmids were digested with *Nde*I and *Hin*dIII, and the released fragments corresponding to the *bla*$_{OXA}$ genes were introduced into *Nde*I/*Hin*dIII digested expression vector pET28a (Novagen, USA), rendering the pET28a/OXAs recombinant plasmids. The identity of the insets was verified by DNA Sanger sequencing. The plasmid constructions were maintained in *E. coli* TOP10 cells and transformed into *E. coli* BL21(DE3) cells for protein expression.

Production and Purification of OXA β-Lactamases. Overnight cultures of recombinant *E. coli* BL21(DE3) producing OXA β-lactamases were diluted (1/50) in 100 mL of fresh LB containing 30 μg/mL kanamycin and cultured at 37 °C until reaching an optical density (OD) of 0.7 at 600 nm. Expression of the β-lactamases genes was carried out at 37 °C for 3 h upon the addition of 0.5 mM isopropyl-β-D-thiogalactopyranoside (IPTG) as an inducer. Bacterial cells were then harvested by centrifugation (30 min at 10000 rpm, 4 °C), resuspended in 10 mL of 25 mM sodium phosphate buffer (pH 7.5), and disrupted by sonication. Debris was eliminated by centrifugation at 13000 rpm for 30 min at 4 °C. Clear supernatants were filtrated through 0.45 μm pore size membranes and then loaded onto HisTrap FF affinity columns (GE Healthcare, USA), previously equilibrated with buffer A (25 mM sodium phosphate buffer, 10 mM imidazole, pH 7.5). The β-lactamase activity was determined qualitatively using nitrocefin hydrolysis. The β-lactamase-containing fractions were eluted with buffer B (25 mM sodium phosphate buffer, 500 mM imidazole, pH 7.5) in a two-step gradient (0−50% and 50−100%). Finally, fractions containing the highest β-lactamase activities were pooled and subsequently dialyzed overnight against 25 mM sodium phosphate buffer (pH 7.5). The His-tag was cleaved by incubating the proteins in the presence of 10 U/mg thrombin (GE Healthcare, USA) at room temperature for 12 h (overnight). Protein purity was estimated by SDS−PAGE in 12% polyacrylamide gels. The fractions of the purified enzymes were stored at −80 °C. All chromatography steps were performed in an ÄKTA Prime Plus purifier (GE Healthcare, USA). The concentration of all protein samples was determined by measuring the absorbance at 280 nm.

Influence of Sodium Bicarbonate in the Activity of OXA Variants. To evaluate the effect of sodium bicarbonate ($NaHCO_3$) in the activity of the OXA β-lactamases, a nanomolar concentration of each variant was mixed with different concentrations of bicarbonate (0 to 100 mM), and the enzyme reaction was launched upon the addition of 100 μM nitrocefin. Velocity rates were recorded for 300 s at room temperature, and initial velocities (v_0) were compared for each $NaHCO_3$ concentration.

Determination of the Steady-State Kinetic Parameters. All the kinetic measurements were performed at 25 °C in 25 mM sodium phosphate buffer (pH 7.5), with or without 50 mM $NaHCO_3$, using a T80 UV−vis spectrophotometer (PG Instruments Ltd., UK). The steady-state kinetic parameters, V_{max} and K_m, were obtained under an initial rate, as described previously,[27] with nonlinear least-squares fitting of the data (Henri Michaelis−Menten equation; eq 1) performed with GraphPad Prism 5.03 for Windows (GraphPad Software, Inc., La Jolla, CA):

https://dx.doi.org/10.1021/acsinfecdis.0c00537
ACS Infect. Dis. XXXX, XXX, XXX−XXX

$$v = \frac{V_{max} \times [S]}{K_m + [S]} \quad (1)$$

For low K_m values, the k_{cat} values were derived by evaluation of the complete hydrolysis time courses as described by De Meester et al.[28] For competitive inhibitors, or poor substrates, the inhibition constant K_i was determined by monitoring the residual activity of the enzyme in the presence of various concentrations of the drug and 100 μM nitrocefin as the reporter substrate;[29] the corrected K_i (considered as the observed or apparent K_m) value is finally determined using the eq 2:

$$K_i = \frac{K_{iobs}}{1 + [S]/K_{m(S)}} \quad (2)$$

where $K_{m(S)}$ and [S] are the reporter substrate's K_m and fixed concentration used, respectively.

The following extinction coefficients and wavelengths were used: nitrocefin ($\Delta\varepsilon^{482}$ = +15000 M^{-1} cm^{-1}), ceftazidime ($\Delta\varepsilon^{260}$ = −9000 M^{-1} cm^{-1}), cefotaxime ($\Delta\varepsilon^{260}$ = −7500 M^{-1} cm^{-1}), imipenem ($\Delta\varepsilon^{300}$ = −9000 M^{-1} cm^{-1}), meropenem ($\Delta\varepsilon^{300}$ = −6500 M^{-1} cm^{-1}), and ertapenem ($\Delta\varepsilon^{300}$ = −12000 M^{-1} cm^{-1}).

Circular Dichroism. Spectra were recorded on a Jasco J-810 spectropolarimeter. Data in the near UV (250−320 nm) or in the far UV (200−250 nm) regions were collected at 25 °C using 10 or 1 mm path length cuvettes, respectively. A scan speed of 20 nm/min with a time constant of 1 s was used for all proteins. Each spectrum was measured at least three times, and the data were averaged to minimize the noise. The molar ellipticity was calculated as described elsewhere,[30] using mean residue weight values of 115.18, 115.15, 114.84, and 115.11 for OXA-48, OXA-163, OXA-247, and OXA-438, respectively.

Thermal Denaturation. Thermal unfolding was monitored by the change of the dichroic signal at 222 nm. The dynode voltage (voltage applied to the photomultiplier tube to compensate for the reduction in the light intensity) was recorded simultaneously. Each protein sample (200 μL, 3 μM) contained in a 1 mm cell cuvette was gradually heated from 25 to 85 °C at a scan rate of 1 °C/min.

For the spectroscopic techniques, phosphate-buffered saline (137 mM NaCl, 2.7 mM KCl, 1.5 mM KH_2PO_4, and 8 mM Na_2HPO_4) was used.

■ ASSOCIATED CONTENT

Supporting Information

The Supporting Information is available free of charge at https://pubs.acs.org/doi/10.1021/acsinfecdis.0c00537.

List of primers used (Table S1), PFGE photo showing the number and size of plasmids harbored by the OXA-producing clinical isolates and transconjugant *E. coli* strains (Figure S1), and schematic view of the plasmid-borne blaOXA genes and their genetic environment (Figure S2) (PDF)

■ AUTHOR INFORMATION

Corresponding Author

Pablo Power − *Consejo Nacional de Investigaciones Científicas y Técnicas (CONICET), Buenos Aires 1452, Argentina; Facultad de Farmacia y Bioquímica, Instituto de Investigaciones en Bacteriología y Virología Molecular (IBaViM), Departamento de Microbiología, Inmunología, Biotecnología y Genética, Laboratorio de Resistencia Bacteriana, Universidad de Buenos Aires, Buenos Aires 1113, Argentina;* orcid.org/0000-0002-7051-9954; Email: ppower@ffyb.uba.ar

Authors

Denise De Belder − *Servicio Antimicrobianos - National Reference Laboratory in Antimicrobial Resistance (NRLAR), Instituto Nacional de Enfermedades Infecciosas-ANLIS "Dr. Carlos G. Malbrán", Buenos Aires 1282, Argentina; Consejo Nacional de Investigaciones Científicas y Técnicas (CONICET), Buenos Aires 1452, Argentina*

Barbara Ghiglione − *Consejo Nacional de Investigaciones Científicas y Técnicas (CONICET), Buenos Aires 1452, Argentina; Facultad de Farmacia y Bioquímica, Instituto de Investigaciones en Bacteriología y Virología Molecular (IBaViM), Departamento de Microbiología, Inmunología, Biotecnología y Genética, Laboratorio de Resistencia Bacteriana, Universidad de Buenos Aires, Buenos Aires 1113, Argentina*

Fernando Pasteran − *Servicio Antimicrobianos - National Reference Laboratory in Antimicrobial Resistance (NRLAR), Instituto Nacional de Enfermedades Infecciosas-ANLIS "Dr. Carlos G. Malbrán", Buenos Aires 1282, Argentina*

Juan Manuel de Mendieta − *Servicio Antimicrobianos - National Reference Laboratory in Antimicrobial Resistance (NRLAR), Instituto Nacional de Enfermedades Infecciosas-ANLIS "Dr. Carlos G. Malbrán", Buenos Aires 1282, Argentina*

Alejandra Corso − *Servicio Antimicrobianos - National Reference Laboratory in Antimicrobial Resistance (NRLAR), Instituto Nacional de Enfermedades Infecciosas-ANLIS "Dr. Carlos G. Malbrán", Buenos Aires 1282, Argentina*

Lucrecia Curto − *Consejo Nacional de Investigaciones Científicas y Técnicas (CONICET), Buenos Aires 1452, Argentina; IQUIFIB, Universidad de Buenos Aires, Facultad de Farmacia y Bioquímica, Buenos Aires 1113, Argentina*

Adriana Di Bella − *Hospital Nacional "Profesor Alejandro Posadas", El Palomar, Buenos Aires 1684, Argentina*

Gabriel Gutkind − *Consejo Nacional de Investigaciones Científicas y Técnicas (CONICET), Buenos Aires 1452, Argentina; Facultad de Farmacia y Bioquímica, Instituto de Investigaciones en Bacteriología y Virología Molecular (IBaViM), Departamento de Microbiología, Inmunología, Biotecnología y Genética, Laboratorio de Resistencia Bacteriana, Universidad de Buenos Aires, Buenos Aires 1113, Argentina*

Sonia A. Gomez − *Servicio Antimicrobianos - National Reference Laboratory in Antimicrobial Resistance (NRLAR), Instituto Nacional de Enfermedades Infecciosas-ANLIS "Dr. Carlos G. Malbrán", Buenos Aires 1282, Argentina; Consejo Nacional de Investigaciones Científicas y Técnicas (CONICET), Buenos Aires 1452, Argentina*

Complete contact information is available at: https://pubs.acs.org/10.1021/acsinfecdis.0c00537

Notes

The authors declare no competing financial interest.

■ ACKNOWLEDGMENTS

This work was funded in part by grants from the University of Buenos Aires (UBACyT 2014-2017 to P.P.) and Agencia Nacional de Promoción Científica y Tecnológica (BID PICT 2014-0457 to P.P.). B. Ghiglione, L. Curto, G. Gutkind, S. Gómez, and P. Power are researchers for the CONICET, Argentina. D. De Belder was a recipient of a PhD fellowship for CONICET.

REFERENCES

(1) Naas, T., Oueslati, S., Bonnin, R. A., Dabos, M. L., Zavala, A., Dortet, L., Retailleau, P., and Iorga, B. I. (2017) β-Lactamase database (BLDB) - structure and function. *J. Enzyme Inhib. Med. Chem. 32*, 917−919.

(2) Antunes, N. T., Lamoureaux, T. L., Toth, M., Stewart, N. K., Frase, H., and Vakulenko, S. B. (2014) Class D β-lactamases: are they all carbapenemases? *Antimicrob. Agents Chemother. 58*, 2119−2125.

(3) Poirel, L., Naas, T., and Nordmann, P. (2010) Diversity, epidemiology, and genetics of class D β-lactamases. *Antimicrob. Agents Chemother. 54*, 24−38.

(4) Stojanoski, V., Chow, D. C., Fryszczyn, B., Hu, L., Nordmann, P., Poirel, L., Sankaran, B., Prasad, B. V., and Palzkill, T. (2015) Structural Basis for Different Substrate Profiles of Two Closely Related Class D β-Lactamases and Their Inhibition by Halogens. *Biochemistry 54*, 3370−3380.

(5) Pitout, J. D. D., Peirano, G., Kock, M. M., Strydom, K. A., and Matsumura, Y. (2019) The Global Ascendency of OXA-48-Type Carbapenemases. *Clin. Microbiol. Rev. 33*, e00102−e00119.

(6) Evans, B. A., and Amyes, S. G. (2014) OXA β-lactamases. *Clin Microbiol Rev. 27*, 241−263.

(7) Bogaerts, P., Naas, T., Saegeman, V., Bonnin, R. A., Schuermans, A., Evrard, S., Bouchahrouf, W., Jove, T., Tande, D., de Bolle, X., Huang, T. D., Dortet, L., and Glupczynski, Y. (2017) OXA-427, a new plasmid-borne carbapenem-hydrolysing class D β-lactamase in *Enterobacteriaceae*. *J. Antimicrob. Chemother. 72*, 2469−2477.

(8) Magagnin, C. M., Rozales, F. P., Antochevis, L., Nunes, L. S., Martins, A. S., Barth, A. L., Sampaio, J. M., and Zavascki, A. P. (2017) Dissemination of bla OXA-370 gene among several *Enterobacteriaceae* species in Brazil. *Eur. J. Clin. Microbiol. Infect. Dis. 36*, 1907−1910.

(9) Oueslati, S., Nordmann, P., and Poirel, L. (2015) Heterogeneous hydrolytic features for OXA-48-like β-lactamases. *J. Antimicrob. Chemother. 70*, 1059−1063.

(10) Poirel, L., Castanheira, M., Carrer, A., Rodriguez, C. P., Jones, R. N., Smayevsky, J., and Nordmann, P. (2011) OXA-163, an OXA-48-related class D β-lactamase with extended activity toward expanded-spectrum cephalosporins. *Antimicrob. Agents Chemother. 55*, 2546−2551.

(11) Poirel, L., Potron, A., and Nordmann, P. (2012) OXA-48-like carbapenemases: the phantom menace. *J. Antimicrob. Chemother. 67*, 1597−1606.

(12) Couture, F., Lachapelle, J., and Levesque, R. C. (1992) Phylogeny of LCR-1 and OXA-5 with class A and class D β-lactamases. *Mol. Microbiol. 6*, 1693−1705.

(13) Docquier, J. D., Calderone, V., De Luca, F., Benvenuti, M., Giuliani, F., Bellucci, L., Tafi, A., Nordmann, P., Botta, M., Rossolini, G. M., and Mangani, S. (2009) Crystal structure of the OXA-48 β-lactamase reveals mechanistic diversity among class D carbapenemases. *Chem. Biol. 16*, 540−547.

(14) Gomez, S., Pasteran, F., Faccone, D., Bettiol, M., Veliz, O., De Belder, D., Rapoport, M., Gatti, B., Petroni, A., and Corso, A. (2013) Intrapatient emergence of OXA-247: a novel carbapenemase found in a patient previously infected with OXA-163-producing *Klebsiella pneumoniae*. *Clin. Microbiol. Infect. 19*, E233−235.

(15) Pasteran, F., Denorme, L., Ote, I., Gomez, S., De Belder, D., Glupczynski, Y., Bogaerts, P., Ghiglione, B., Power, P., Mertens, P., and Corso, A. (2016) Rapid identification of OXA-48 and OXA-163 subfamily in carbapenem resistant gram-negative bacilli with a novel immunochromatographic lateral flow assay. *J. Clin. Microbiol. 54*, 2832−2836.

(16) Maveyraud, L., Golemi, D., Kotra, L. P., Tranier, S., Vakulenko, S., Mobashery, S., and Samama, J. P. (2000) Insights into class D β-lactamases are revealed by the crystal structure of the OXA-10 enzyme from *Pseudomonas aeruginosa*. *Structure 8*, 1289−1298.

(17) Golemi, D., Maveyraud, L., Vakulenko, S., Samama, J. P., and Mobashery, S. (2001) Critical involvement of a carbamylated lysine in catalytic function of class D β-lactamases. *Proc. Natl. Acad. Sci. U. S. A. 98*, 14280−14285.

(18) Benjwal, S., Verma, S., Rohm, K. H., and Gursky, O. (2006) Monitoring protein aggregation during thermal unfolding in circular dichroism experiments. *Protein Sci. 15*, 635−639.

(19) Angelani, C. R., Caramelo, J. J., Curto, L. M., and Delfino, J. M. (2017) Structural coalescence underlies the aggregation propensity of a beta-barrel protein motif. *PLoS One 12*, No. e0170607.

(20) Tien, M., Berlett, B. S., Levine, R. L., Chock, P. B., and Stadtman, E. R. (1999) Peroxynitrite-mediated modification of proteins at physiological carbon dioxide concentration: pH dependence of carbonyl formation, tyrosine nitration, and methionine oxidation. *Proc. Natl. Acad. Sci. U. S. A. 96*, 7809−7814.

(21) Clinical and Laboratory Standards Institute. (2018) *Performance standards for antimicrobial susceptibility testing; twenty-eight informational supplement M100-S28*, Vol. *38*, Clinical and Laboratory Standards Institute, Wayne, PA.

(22) Pasteran, F., Gonzalez, L. J., Albornoz, E., Bahr, G., Vila, A. J., and Corso, A. (2016) Triton Hodge Test: Improved Protocol for Modified Hodge Test for Enhanced Detection of NDM and Other Carbapenemase Producers. *J. Clin. Microbiol. 54*, 640−649.

(23) Gomez, S. A., Pasteran, F. G., Faccone, D., Tijet, N., Rapoport, M., Lucero, C., Lastovetska, O., Albornoz, E., Galas, M., Group, K. P. C., Melano, R. G., Corso, A., and Petroni, A. (2011) Clonal dissemination of *Klebsiella pneumoniae* ST258 harbouring KPC-2 in Argentina. *Clin. Microbiol. Infect. 17*, 1520−1524.

(24) Barton, B. M., Harding, G. P., and Zuccarelli, A. J. (1995) A general method for detecting and sizing large plasmids. *Anal. Biochem. 226*, 235−240.

(25) Carattoli, A., Bertini, A., Villa, L., Falbo, V., Hopkins, K. L., and Threlfall, E. J. (2005) Identification of plasmids by PCR-based replicon typing. *J. Microbiol. Methods 63*, 219−228.

(26) Carattoli, A. (2009) Resistance plasmid families in *Enterobacteriaceae*. *Antimicrob. Agents Chemother. 53*, 2227−2238.

(27) Segel, I. H. (1975) Rapid equilibrium partial and mixed-type inhibition. In *Enzyme kinetics, behavior and analysis of rapid equilibrium and steady-state enzyme systems*, pp 208−224, John Wiley & Sons, Inc., New York, NY.

(28) De Meester, F., Joris, B., Reckinger, G., Bellefroid-Bourguignon, C., Frere, J. M., and Waley, S. G. (1987) Automated analysis of enzyme inactivation phenomena. Application to β-lactamases and DD-peptidases. *Biochem. Pharmacol. 36*, 2393−2403.

(29) Power, P., Di Conza, J., Rodriguez, M. M., Ghiglione, B., Ayala, J. A., Casellas, J. M., Radice, M., and Gutkind, G. (2007) Biochemical characterization of PER-2 and genetic environment of bla_{PER-2}. *Antimicrob. Agents Chemother. 51*, 2359−2365.

(30) Schmid, F. (1989) Optical spectroscopy to characterize protein conformation and conformational changes. In *Protein Structure: a practical approach* (Creighton, T. E., Ed.), pp 261−296, IRL, New York, NY.

https://dx.doi.org/10.1021/acsinfecdis.0c00537
ACS Infect. Dis. XXXX, XXX, XXX−XXX